Gold nanoparticle assays: towards single molecule unamplified DNA detection

R. Verdoold*, F. Ungureanu, D. Wasserberg and R. P. H. Kooyman
University of Twente, MESA+ Institute, Biophysical Engineering Group,
P.O. Box 217, 7500 AE Enschede, the Netherlands

ABSTRACT

The light scattering and absorption properties of gold nanoparticles (GNPs) can be utilised for the detection of DNA. Binding of molecules to the GNP influences the local refractive index. The increase in refractive index can be measured as proportional red-shift of the GNPs extinction maximum; therefore GNPs are suitable for use as nanoparticle chemical sensors. Utilizing this method it is possible to detect DNA in naturally occurring quantities.

In bulk measurements we have shown a red-shift of 7 nm of the absorption maximum (λ_{max}) upon binding of thiolated ssDNA. Subsequently, we were able to follow the interaction between two sets of GNPs functionalised with complementary strands.

Randomly immobilised GNPs were visualised with an inverted darkfield microscope. The use of a colour camera enables us to analyse the colour change of each individual particle in the field of view. A change of λ_{max} of 1 nm can be detected by the colour camera, which corresponds to ~100 20mer ssDNA molecules. For the detection of a single DNA binding events we are developing an assay for DNA detection, utilizing a second set of GNPs. The interaction of two GNPs within a range of 2.5 times the radius of each other results in a shift of ~7 nm in λ_{max} for the presence of one DNA strand. This increased shift makes the method not only more accurate but also easier to detect.

Keywords: Optical detection, Gold nanoparticles, Single molecule, unamplified DNA detection

1. INTRODUCTION

In many assay formats, the detection of specific DNA sequences requires the use of optical probes mostly based on fluorescence, colorimetry, chemiluminescence or radioactive isotopes [1, 2]. These probes are used as direct or indirect labels. Most detection approaches, as those based on the real-time polymerase chain reaction and microarrays, operate on the basis of obtaining cumulative signal of multiple labels. It is very hard for both methods to detect near single molecule binding events; furthermore both methods require the use of specific amplified DNA. Besides the disadvantages of using fluorescent probes like photobleaching and quenching a complexes apparatus built from expensive components is necessary. Fluorescent detection is still one of the most favourable method for DNA detection at the moment.

Noble metal nanoparticles functionalised with DNA receptor strands do not have these limitations [3]. Introduced in 1996 oligonucleotide functionalised gold nanoparticles (GNPs) [4] have extensively been studied for applications in diagnostics and fields as intracellular RNA quantification [5] as well as gene regulation [6]. When GNPs are placed in an electromagnetic field with a well-defined resonant wavelength (λ_{max}) localised surface plasmons can be excited [7, 8]. At resonance, the scattering cross section of a single GNP with a diameter of 60 nm is 10^5 times larger than that of a fluorescein molecule at the same conditions. Therefore single GNPs can easily be visualized with darkfield microscopy in combination with simple detection equipment e.g. a CCD-camera.

The wavelength of the excited surface plasmon of the nanoparticle depends on its composition, size and shape, and the refractive index of the local environment. Refractive index changes of the local environment result in a direct change of the extinction maximum, making noble metal nanoparticles suitable for local refractive index sensing. The local refractive index of the GNP will change if molecules bind to the GNP surface. This is the basis for their potential use as chemical sensors for the detection of e.g. DNA or proteins. The distance over which the GNP can detect changes in local refractive index extends to the order of 10 nanometers around the particle.

* r.verdoold@utwente.nl ; Phone +31-(0)53-489 1080; +31-(0)53-489 1105, http://bpe.tnw.utwente.nl

Advanced Environmental, Chemical, and Biological Sensing Technologies VI
edited by Tuan Vo-Dinh, Robert A. Lieberman, Günter Gauglitz, Proc. of SPIE Vol. 7312
73120N · © 2009 SPIE · CCC code: 0277-786X/09/$18 · doi: 10.1117/12.818120

We choose to use DNA for our detection purposes for a number of reasons: (i) DNA has successfully been conjugated to GNPs for 10 years [4]; (ii) specific DNA target detection using plasmon coupling has been shown for experiments performed in solution [9, 10]; (iii) the length of the ssDNA receptor strand can be chosen and controlled [11], also DNA is quite stable in comparison with proteins which makes it relatively easy to handle in (buffer) solutions; (iv) the approach for DNA conjugation and detection is generic, thus different sequences can be conjugated following nearly identical protocols; (v) the detection of single DNA binding events is relevant for applications in industry, lifesciences and biomedical technology [12, 13].

In this paper we explore the use of oligonucleotide functionalised GNPs as sensor platform.

2. THEORETICAL BACKGROUND

As has been described by Hill et al. [14], and Hurst et al. [15], a 60 nm GNP can host up to ~900 ssDNA molecules. Using this amount we simulated the local refractive index change upon binding of 20mer ssDNA molecules. From discrete dipole scattering simulations for 60 nm GNPs we conclude that the binding of ~125 of these ssDNA that have a length of ~7 nm results in a wavelength shift of 1 nm as is shown in fig. 1.

Thus, for a single GNP with 500 active receptor strands our detection limit (Γ_{min}) is a quarter of the available binding sites (Γ_{min} =0.25) assuming that we can detect a 1 nm shift. With an affinity constant of $2.0 \cdot 10^7$ M^{-1} for a 16mer ssDNA [16] and assuming Langmuir type behaviour this would result in a theoretical detection limit of ~20 nM. The usage of a single GNP for label free DNA detection is therefore relatively limited. However when we hybridise with a second DNA-GNP within a range of 20 nm from the first particle an enhanced effect is created. The interaction between the particles as the result of a single target hybridisation event results in a shift of approximately 8 nm as illustrated in Figure 2. Thus if we would be able to observe 250 GNPs simultaneously, of which each accommodates 500 active receptors we could theoretically detect 1 out of 125,000 binding sites ($\Gamma_{min} = 8.0 \cdot 10^{-6}$). The particle-particle interaction has been shown by Sönnichsen et al. who demonstrated a significant shift of λ_{max} upon binding of one particle within the plasmon field [17]. In Figure 3 the principle of the so-called sandwich assay is illustrated. As can be seen from figure 3 the resulting distance between two GNPs after hybridisation is determined by the length of the DNA strands coupled to both GNPs and the degree of overlap that is chosen for the target DNA strand.

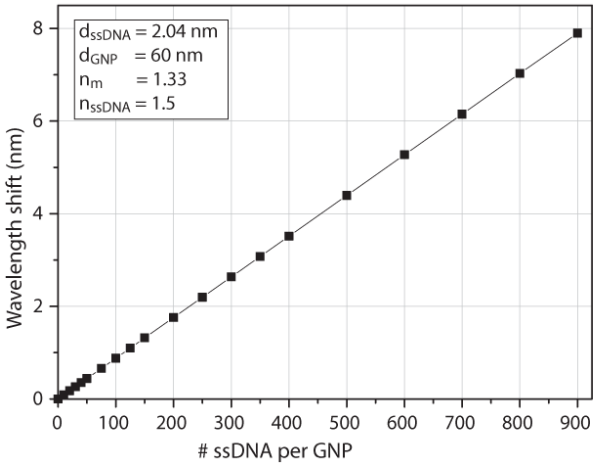

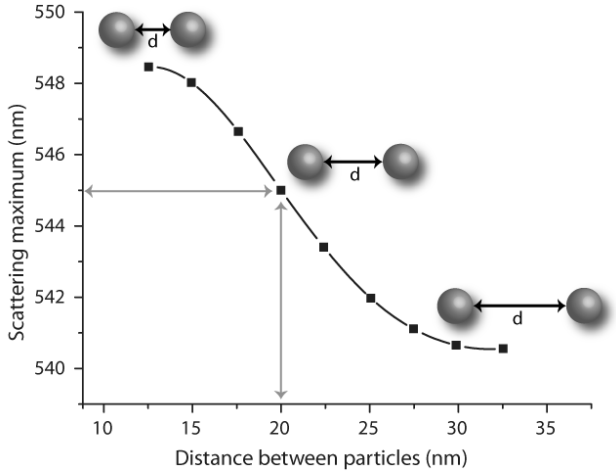

Fig. 1 Left. Simulation where 20mer ssDNA, with ~7 nm length, binds to a 60 nm GNP.

Fig. 2 Right. Theoretical λ_{max} as a function of distance between two 60 nm diameter GNPs in water.

The sensing approach illustrated in fig. 3 can easily be extended to a multiplex assay by using different sized or shaped GNPs. The λ_{max} is unique for each type of particle based on shape, size and material. Using a colour camera we can monitor and discriminate individual groups of particles by their scattering colour. However the ability of multiplexing detection reduces the overall sensitivity of the system, due to the decreased number of GNPs for each type of strand in a multiplexed assay resulting in a increased Γ_{min}.

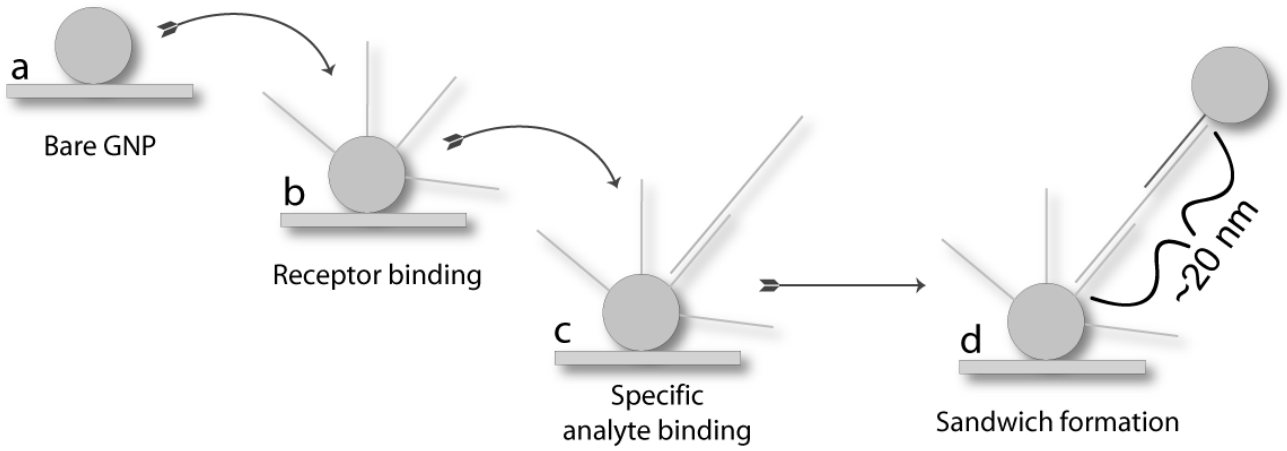

Fig. 3. Schematic representation of surface binding assay; (a) bare GNPs are immobilised on a glass substrate; (b) receptor molecules bind to the GNPs, the change of λ_{max} is proportional to the amount of receptor molecules bound to each GNP; (c) after washing the sample is incubated with target DNA; (d) after a second washing step only specifically bound target strands remain bound to the GNPs. Incubation with a second complementary DNA-GNP conjugate results in sandwich complexes.

3. MATERIALS & METHODS

3.1. Materials

Citrate capped GNPs were purchased from British Biocell International (Cardiff, UK). Thiolated oligonucleotides were purchased from Eurogentec S.A. (Seraing, Belgium). Dithiothreitol (DTT), 3-aminopropyltriethoxysilane (APTES), salts and reagents were purchased from Sigma-Aldrich (St. Louis, MO, USA). Illustra NAP-5 mini spincolumns containing a Sephadex G-25 DNA grade matrix were purchased from G.E. Healthcare UK limited (Buckinghamshire, UK). Quartz cuvettes (8 channel and single channel) and Hellmanex 2 cleaning solution were purchased from Hellma GmbH. (Müllheim, Germany). All aqueous solutions were made from purified water (MiliQ) (> 18.2 MΩ/cm) with a Millipore Academic purifier (Billerica, MA, USA). Aqueous solutions were degassed prior to usage.

3.2. Instrumentation

Spectrophotometric analyses of DNA, GNPs and conjugates in solution were carried out on a Shimadzu UV-2401PC UV-Vis spectrophotometer. A Shimadzu TMSPC 8 peltier controlled thermostat was used for melting and hybridisation experiments. Nitrogen gas was used to prevent condensation on the outside of the cuvette at temperatures below ambient. For GNP imaging an Olympus GX71 inverted microscope with an MPLAN 20x darkfield objective in combination with a 75 watt xenon lamp as a light source was used. A true-colour Zeiss Axiocam HRc camera was used to acquire images with 14 bit colourdepth. An Ocean Optics QE65000 fibre spectrophotometer was attached to the microscope to obtain spectral information of single GNPs. Sonications were carried out using a Branson 2510 sonicator. The flowspeed was controlled using a World precision instruments Aladdin-1000 syringe pump. Electron microscopy was carried out using a Philips XL30 environmental scanning electron microscopy (ESEM).

3.3. Sequence design

For these investigations ssDNA sequences A, B and A' were designed to have a length of 20 oligonucleotides. Strands A and B are 5' thiol modified and the strand A' complementary to A over 18 bases has a 3' thiol modification. There is also a middle strand M consisting of 56 oligonucleotides capable of hybridising both DNA A and B over 18 bases. The 18 bases overlap is chosen to have a 2 base spacer at the thiol side. In table 1 the DNA strand information is shown. When hybridised A/A' and A/M have an EcoR1 restriction site, which can be used to free hybridised particles with an irreversible enzymatic reaction.

Table 1. DNA strand information.

Name	Linker	Sequence 5' → 3'	Melting point (found for 250 mM NaCl buffer)
A	Thiol 5'	GCA GAC TTG GAA TTC GCG CC	~73 ºC with A' or part of M
B	Thiol 5'	CCC CCC AAG CTT GAT CAT GC	~74 ºC with part of M
A'	Thiol 3'	ACG GCG CGA ATT CCA AGT CT	~73 ºC with A
M	-	ATG ATC AAG CTT GGG GGG GAG AGA GAG AGG CCA ACA ACG GCG CGA ATT CCA AGT CT	See other strands

3.4. Preparation of oligonucleotide-functionalised gold nanoparticles

The functionalisation of GNPs with oligonucleotides was performed using modified methods from literature [15]. Prior to conjugation the protecting disulfide groups on the oligonucleotides were cleaved using a DTT solution. A volume of 100 µM ssDNA was mixed with an equal volume of 340 mM phosphate buffer (PB) at pH 8.0. Subsequently, DTT was added to a final concentration of 100 mM. Samples were incubated on a orbital shaker for 2 hours at room temperature (RT) followed by a washing step using a MiliQ rinsed NAP-5 centrifuge column. The yield of this step was between 80 and 90%. The samples were diluted to 5 µM with MiliQ and heated to 96ºC for 10 minutes to ensure single strand conformation.

A solution was made by mixing NaCl, sodium dodecyl sulphate (SDS), PB at pH 7.4 and ssDNA. This was incubated for 15 minutes and followed by the addition of 1 ml GNP stock solution ($3.6 \cdot 10^{-11}$ M) resulting in a 10 ml mixture with final concentrations of 500 mM NaCl, 10 mM PB at pH 7.4, 0.01 (wt/vol) % SDS and oligonucleotides at 20,000 copies per GNP. The samples were incubated on a rotator at RT for 24 hours followed by several washing steps.

Subsequently, samples were pelleted by centrifugation for an hour at 3900x g and the supernatant was replaced by 10 ml washing solution (0.01% SDS in MiliQ water). This step was repeated twice. In the second step the samples were resuspended in 1 ml and transferred to containers. Subsequently, 3 more washing steps were done at 15,000x g for 20 minutes replacing the supernatant with 1 ml washing solution. To resuspend the pellet from the bottom the samples were sonicated for 10 seconds whilst shaken. The colloidal solutions of DNA-GNPs were stored at 4ºC until further usage. Conjugation quality was checked with the spectrophotometer in visible light (cf. section 4.1).

3.5. In solution hybridisation and melting analysis of oligonucleotide-functionalised gold nanoparticles

To boost the concentration before usage DNA-GNPs solutions were centrifuged and resuspended in half the original volume. Samples of 150 µl were made containing 250 mM NaCl, 0.01% SDS, 10 mM PB with pH 7.2, MiliQ water and 100 µl GNP solution. Samples containing the hybridisation pair DNA-A-GNP / DNA-A'-GNP had 50 µl of each DNA-GNP solution. Samples were mixed and incubated in a drybath at 96ºC for 10 minutes. Subsequently, the block with samples was removed and cooled down to room temperature in 2 hours. Samples were vortexed and transferred to cuvettes for melting point analysis. The temperature was ramped from 4ºC to 96ºC at a rate of 0.2ºC / minute. Each 0.5ºC the absorbance was measured at λ = 260 nm. The temperature was held at 96ºC for 10 minutes at the end of the cycle. Subsequently, the measurement was continued by decreasing the temperature to 4ºC at a rate of 0.2ºC / minute.

3.6. Gold nanoparticle immobilisation and flowcell fabrication for darkfield microscopy

GNPs were immobilised on an APTES coated glass slide. These slides were prepared using modified literature methods [18, 19] . Menzel (Braunschweig, Germany) BK7 coverslips (76 x 26 mm) were placed in a glass holder and incubated in piranha solution (1 H_2O_2 (35%) : 3 H_2SO_4 (>96%)) at 95ºC for 15 minutes (Caution, piranha solution is highly corrosive). After cleaning the slides were transferred to MiliQ water and washed twice, followed by a 15 minute incubation in a 5% APTES solution diluted in 99.9% ethanol. Subsequently, slides were sonicated in fresh MiliQ water 3 times for 5 minutes. After washing the silanisation was finalised by a 3 hour baking step at 120ºC. Slides were stored at this temperature for a maximum of 2 days. Storage longer than 2 days results in reduced adhesion of GNPs. After baking or storage each slide was cooled to room temperature (RT) and incubated with a 50x diluted GNP stock solution in MiliQ ($4.4 \cdot 10^9$ particles/ ml) for 5 minutes in a petridish while shaking at 50 rpm. Subsequently, slides were washed once with MiliQ and dried with nitrogen gas and used.

A flowcell was made by using the coverslip with GNPs as base plate followed by a mould cut parafilm covered with a microscope object slide with holes fabricated for fluid connectors. The three pieces were placed onto each other and

heated to 80ºC on a hot plate. This procedure melts the parafilm gluing both slides together. The channels cut out from the parafilm acted as flowcell channels and had a volume of 28 µl.

3.7. Single gold nanoparticle analysis on surface

The flowcell was washed with a buffer consisting of 250 mM NaCl and 10 mM PB pH 7.4 followed by incubation in flow with ssDNA A. The DNA A was DTT treated as described above and diluted to 2.5 µM in a 500 mM NaCl aqueous solution. Prior to incubation the DNA was heated to 96ºC for 10 minutes and rapidly cooled down on ice. After the ssDNA incubation step the flowcell was washed with buffer and incubated with strand M at 2.5 µM in 250 mM NaCl aqueous solution. Subsequently, the flowcell was washed again with buffer followed by the final incubation with DNA B-GNPs at 10 nM (GNPs) in 250 mM NaCl in aqueous solution. After the final incubation step the flowcell was washed with buffer.

During the experiment images were continuously acquired at 1 minute intervals. RAW image information was stored with subsequent numbering followed by analyses using an in house developed MatLab code [8].

3.8. Image analysis

From an image a region of interest is selected containing a single GNP, and subsequently the pixel intensity values for the three colour channels are determined. In an earlier study [8] we described the use of the change in ratio of the red channel over the green channel (r/g) to express a shift in wavelength maximum. It was found that the use of this method allows us to detect changes in λ_{max} of ~1 nm with the instrument described in section 3.2. This corresponds to a binding of ~100 20mer ssDNA molecules.

4. RESULTS AND DISCUSSION

4.1. Oligonucleotide-functionalised gold nanoparticles

In figure 4 the change in λ_{max} as the result of DNA A binding to 60 nm GNPs is shown. A high ionic strength buffer (>500 mM NaCl) is necessary to successfully conjugate ssDNA to GNPs. However GNPs are instable in these solutions. To reduce GNP aggregation a high concentration of ssDNA (>20,000 copies per GNP) in a large volume was used. Under these conditions aggregation was minimal as judged from the shape of the curve in Figure 4. If GNP aggregation occurs a second peak is visible at $\lambda > 600$ nm. The shift that we obtained for the coupling of 20mer ssDNA was ~7 nm which corresponds to a theoretical amount of ~900 ssDNA molecules per GNP. An increased length of the ssDNA resulted in a larger shift, because the DNA shell thickness has increased (data not shown).

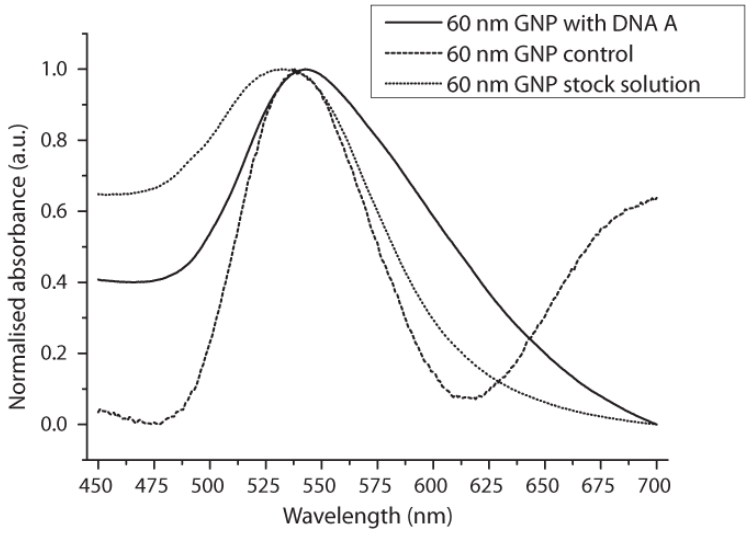

Fig. 4. Absorbance curves of GNPs; the 20mer ssDNA A (~7 nm) conjugation shows a shift when compared to the stock GNP solution. The control sample without ssDNA shows aggregation of GNPs in view of the observed increase of absorbance at $\lambda > 600$ nm.

4.2. In solution hybridisation and melting analysis of oligonucleotide-functionalised gold nanoparticles

Measurements in solution were performed with both increasing and decreasing temperatures. Prior to the hybridisation and melting analysis of DNA-GNPs the melting temperature (Tm) was determined for the hybridisation of free DNA-A and DNA-A'. This was done by measuring the increase in absorbance upon the transition of DNA from double strand to single stranded DNA conformation at λ = 260 nm and vice versa. At Tm half of the DNA has the double strand conformation and half the single strand. At 250 mM of NaCl used for the DNA-GNP conjugates we found a Tm of ~73ºC for the hybridisation of the pair described above. This number was also found from calculations [20, 21] on the employed strand.

The DNA-GNP conjugation pair A and A' aggregated when the temperature of the solution was lowered below Tm. This was visible by a change from a red coloured to a colourless solution. The results of hybridisation of DNA-A-GNP and DNA-A'-GNP are shown in Figure 5a. Subsequently, the samples were melted as shown in Figure 5b. This process of melting and annealing is reversible and could be repeated several times.

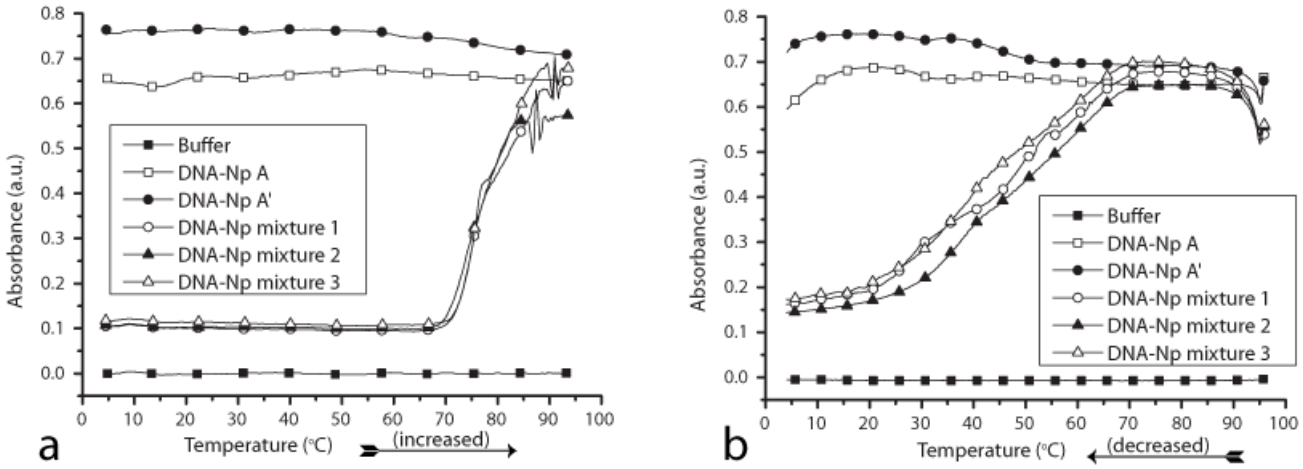

Fig. 5a, 5b. Increasing the temperature results in the melting of DNA, from Tm the DNA strands dehybridise and GNPs return to solution; (b) Decreasing temperatures result in hybridisation of DNA strands attached to GNPs. DNA-GNP mixtures are a combination of 50% DNA-A-GNP and 50% DNA-A'-GNP measured in triplicate.

To this we should add that the temperature induced changes at 260 nm originate from the combined effects of (de)hybridising DNA and precipitating/resuspending GNPs. These experiments show that we can conjugate ssDNA molecules to GNPs which are still capable of reacting with the complementary ssDNA molecule.

4.3. Gold nanoparticle immobilisation

Immobilised bare GNPs were checked under darkfield conditions for their density and colour. In Figure 6a we show a typical darkfield image. When particles were uniformly distributed the flowcell was assembled. From ESEM measurements we infer that particles are not aggregated and uniformly distributed on the surface, as can be seen in Figure 6b. Darkfield measurements can resolve single particles when they are at least 2 µm apart from each other.

GNPs are bound electrostatically to the amino surface; high voltage ESEM (20 KV at 5 torr water pressure), and flowing high ionic strength buffer through the flowcell have shown that GNPs can not be washed off under the experimental conditions employed here.

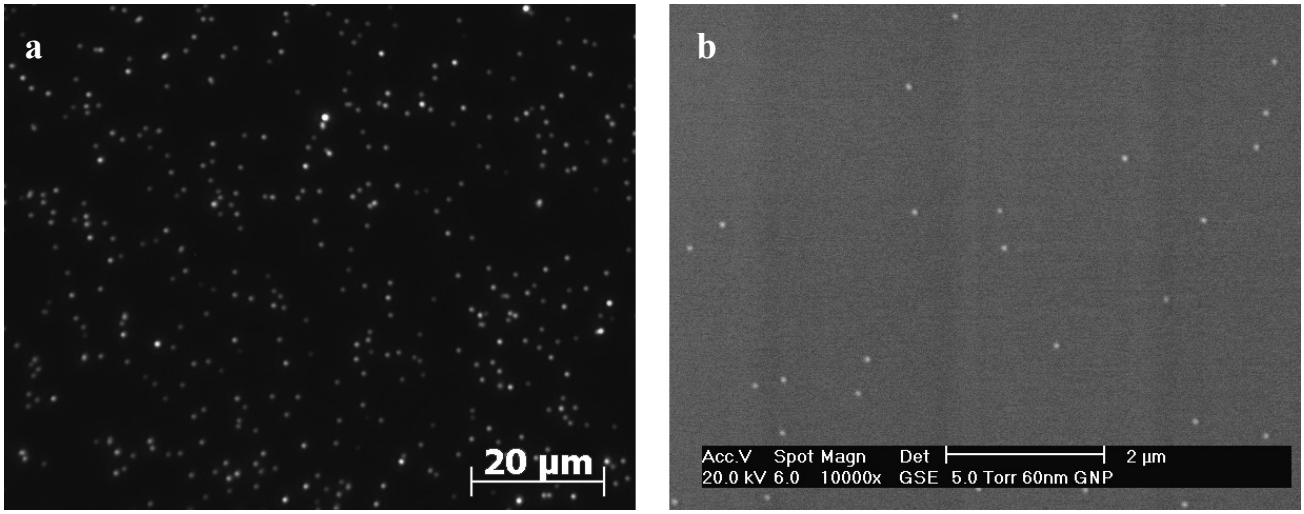

Fig. 6a. Typical darkfield image of randomly immobilised 60 nm GNPs.

Fig. 6b. Typical ESEM image of BBI 60 nm GNPs immobilised on APTES coated glass slide

The storage of APTES coated slides affected the adhesion of GNPs: after 48 hours of storage a prolonged incubation time was necessary. For experiments fresh slides were made within 48 hours prior to the measurement. Aggregation problems occurred when directly after APTES coating the slides were not washed properly. Surfaces of slides prepared without APTES baking resulted in more background structures, making the slides unsuitable for darkfield detection.

4.4. Single gold nanoparticle darkfield analysis on a surface

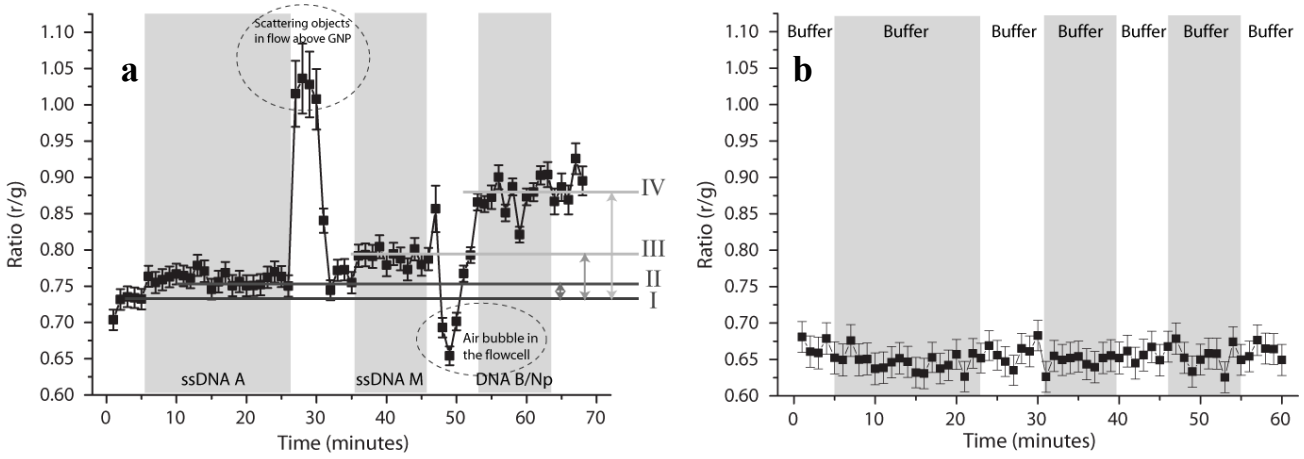

Fig. 7a. Single GNP assay. (I) response from bare GNP on the surface, (II) the response increases after incubated with DNA. Incubation with target strand M (III) increases the response further, and finally (IV) the incubation with the second GNP-B-DNA to form a sandwich increases the response significantly.

Fig. 7b Typical response from a single nanoparticle in the control experiment.

Figure 7a shows preliminary results of a single GNP analysed with the MatLab code. As already mentioned in section 3.8, the shift of λ_{max} can be conveniently expressed in the shift of r/g, which is in the vertical scale in figs. 7a & 7b. Earlier we have determined [8] that $(\Delta r/g) / (\Delta\lambda_{max}) \approx 0.04$ /nm. To obtain a baseline the flowcell was run with buffer at $0 < t < 5$ min. with a flowrate of 25 µl/min. Subsequently, ssDNA-A was flown through the cell at $5 < t < 26$ minutes, the binding of the receptor ssDNA-A to the GNP results in a change $\Delta r/g \approx 0.04$, corresponding to $\Delta\lambda \approx 1$ nm. From discrete dipole scattering simulations we have found that for this size of DNA molecule this is a binding of approximately 100 ssDNA molecules. At $26 < t < 36$ min. the flowcell was washed with buffer and subsequently incubated with the intermediate strand (M) at $36 < t < 46$ min; this resulted in an additional wavelength shift. Again the flowcell was

washed with buffer. At t = 46 min the buffer flow was replaced with a solution of DNA-B-GNP. The binding of this second DNA-B-GNP resulted in a 7 nm shift which is expected in view of the ~20 nm distance of the two GNPs (cf. fig. 2). The shift remains in the last washing step. The fluctuation of the r/g value after the binding of the second particle can be explained by the circumstance that the DNA is a flexible linker allowing movement of the second particle which affects the wavelength shift of the GNP-pair. Sannomiya et al. [22] described a similar effect in their GNP sandwich system.

In a control flowcell measurement shown in Figure 7b only buffer was run. The buffer was exchanged for the same buffer from other containers to simulate change of samples as that might influence the signal. No large effects could be seen from this measurement concluding that the system is stable, and that the effects shown in fig. 7a are DNA induced.

Time traces of single GNPs as depicted in fig. 7a only represent a fraction of the available data. We were able to obtain information for each individual particle in the whole field of view; we observed particles that do not show any response from DNA present. Apart from the possibility that the actual affinity constant is not high enough to bind all available sites another explanation for this is that their binding area might be occupied or not able to bind molecules due to surface impurities.

We find that our detection method is highly sensitive to impurities in solutions or air bubbles in the flowsystem. To this end the use of various surfactants needs to be studied as well as their effect on the hybridisation efficiency.

5. CONCLUSION

In summary, this work shows that the use of a simple darkfield microscope setup in combination with a colour camera can be used to follow a GNP surface binding process as well as its quantification.

The DNA functionalisation shown in this study proves the possibilities of hybridisation between two functionalised GNPs to form a sandwich complex. When only one GNP is used it is possible to measure the binding of the target strand; however, the detection limit is much higher. The sandwich assay overcomes this problem: when two particles are bound together the change in wavelength shift is much larger, as shown by Reinhard and co-workers [23].

At this stage it is difficult to make statements on the number of DNA-B-GNP conjugates that is bound in fig. 7a. To this end further experiments are necessary, as well as the implementation of a statistical analysis of the coverage of a large number of immobilised GNPs.

Our approach using a colour camera with a relatively large field of view, as described here, appears to be an excellent tool for such parallel analysis, providing the experimental data for further statistical analysis.

6. ACKNOWLEDGEMENTS

This research was financially supported by MicroNed (project WP2F-FoaC) and the European Union as a part of the Fluoromag project (FP6-STREP # 037465).

REFERENCES

[1] Nath, N., and Chilkoti, A., "Label free colorimetric biosensing using nanoparticles," J Fluoresc, 14(4), 377-389 (2004).

[2] Schultz, S., Smith, D. R., Mock, J. J. and Schultz, D. A., "Single-target molecule detection with nonbleaching multicolour optical immunolabels," PNAS, 97(3), 996-1001 (2000).

[3] Fritzsche, W. and Taton, T. A., "Metal nanoparticles as labels for heterogenous chip-based DNA detection," Nanotech. 14, R63-R73 (2003).

[4] Mirkin, C. A., Letsinger, R. L., Mucic, R. C. and Storhoff, J. J., "A DNA-based method for rationally assembling nanoparticles into macroscopic materials, " Nature 382(6592), 607-609 (1996).

[5] Seferos, D. S., Giljohann, D. A., Hill, H. D., Prigodich, A. E. and Mirkin, C. A., "Nano-flares: probes for transfection and mRNA detection in living cells," J Am Chem Soc 129(50), 15477-15479 (2007).

[6] Giljohann D. A., Seferos, D. S., Prigodich, A. E., Patel, P. C. and Mirkin, C. A., "Gene regulation with polyvalent siRNA-nanoparticle conjugates," J Am Chem Soc. 131(6), 2072-2073 (2009).
[7] Okamoto, T., Yamaguchi, I. and Kobayashi, T., "Local Plasmon sensor with gold colloid monolayers deposited upon glass substrates," Opt Lett. 25(6), 372-374 (2000).
[8] Ungureanu, F., Halamek, J., Verdoold, R. and Kooyman, R. P. H., "The use of a colour camera for quantitative detection of protein-binding nanoparticles," Proc. SPIE, 7192-23 (2009).
[9] Storhoff, J. J., Lucas, A. D., Garimella, V., Bao, Y. P. and Muller, U. R., "Homogeneous detection of unamplified genomic DNA sequences based on colorimetric scatter of gold nanoparticle probes," Nat. Biotechnol, 22, 883-887 (2004).
[10] Elghanian, R., Storhoff, J. J., Mucic, R. C., Letsinger, R. L. and Mirkin, C. A., "Selective colorimetric detection of polynucleotides based on the distance-dependent optical properties of gold nanoparticles," Science 277, 1078- 1080 (1997).
[11] Smith, S. B., Cui, Y. and Bustamante, C., "Overstretching B-DNA: the elastic response of individual double-stranded and single-stranded DNA molecules," Science.271(5250),795-799 (1996).
[12] Singh-Zocchi, M., Dixit, S., Ivanov, V. and Zocchi, G., "Single-molecule detection of DNA hybridization," Proc Natl Acad Sci, 100(13), 7605-7610 (2003).
[13] Hagan, M. F. and Chakraborty, A. K., "Hybridization dynamics of surface immobilized DNA," J Chem Phys., 120(10), 4958-4968 (2004).
[14] Hill, H. D., Millstone, J. E., Banholzer, M. J. and Mirkin, C. A., "The Role Radius of Curvature Plays in Thiolated Oligonucleotide Loading on Gold Nanoparticles," ACS Nano 3(2), 418-424 (2009).
[15] Hurst, S. J., Lytton-Jean, A. K. and Mirkin, C. A., "Maximizing DNA loading on a range of gold nanoparticle sizes," Anal. Chem. 78(24), 8313-8318 (2006).
[16] Wark, A. W., Lee, H. J. and Corn, R. M., "Long-range surface Plasmon resonance imaging for bioaffinity sensors," Anal. Chem. 77(13), 3904-3907 (2005).
[17] Sönnichsen, C., Reinhard, B. M., Liphardt, J. and Alivisatos, A. P., "A molecular ruler based on plasmon coupling of single gold and silver nanoparticles," Nat. Biotechnol., 23(6), 741-745 (2005).
[18] Festag, G., Steinbruck, A., Wolff, A., Csaki, A., Moller, R. and Fritzsche, W., „Optimization of gold nanoparticle-based DNA detection for microarrays," J Fluoresc., 15, 161-170 (2005).
[19] Crampton, N., Bonass, W. A., Kirkham, J. and Thomson, N. H., "Formation of aminosilane-functionalized mica for atomic force microscopy imaging of DNA. Langmuir, 21, 7884-7891 (2005).
[20] Kibbe, W. A., "OligoCalc: an online oligonucleotide properties calculator," Nucleic Acids Research, Vol. 35, No. suppl_2 W43-W46 (2007).
[21] Long, H., Kudlay, A. and Schatz, G. C., "Molecular dynamics studies of ion distributions for DNA duplexes and DNA clusters: Salt effects and Connection to DNA melting," J. Phys. Chem. B, 110, 2918-2926 (2006).
[22] Sannomiya, T., Hafner, C. and Voros, J., "In situ sensing of single binding events by localized surface plasmon resonance," Nano Lett., 8(10), 3450-3455 (2008).
[23] Reinhard, B. M., Siu, M., Agarwal, H., Alivisatos, A. P. and Liphardt, J., "Calibration of dynamic molecular rulers based on Plasmon coupling between gold particles," Nano Lett. 5(11), 2246-2252 (2005).